

Exact Solution to the Problem of Nonlinear Pulse Propagation through Random Layered Media and its Connection with Number Triangles

Adam Sokolow and Surajit Sen*

Department of Physics, State University of New York, Buffalo, New York 14260-1500

(Dated: May 1, 2007)

Abstract

An energy pulse refers to a spatially compact energy bundle. In nonlinear pulse propagation, the nonlinearity of the relevant dynamical equations could lead to pulse propagation that is non-dispersive or weakly dispersive in space and time. Nonlinear pulse propagation through layered media with widely varying pulse transmission properties is not wave-like and a problem of broad interest in many areas such as optics, geophysics, atmospheric physics and ocean sciences. We study nonlinear pulse propagation through a semi-infinite sequence of layers where the layers can have arbitrary energy transmission properties. By assuming that the layers are rigid, we are able to develop exact expressions for the backscattered energy received at the surface layer. The present study is likely to be relevant in the context of energy transport through soil and similar complex media. Our study reveals a surprising connection between the problem of pulse propagation and the number patterns in the well known Pascal's and Catalan's triangles and hence provides an analytic benchmark in a challenging problem of broad interest. We close with comments on the relationship between this study and the vast body of literature on the problem of wave localization in disordered systems.

PACS numbers: 05.10.-a,05.45.-a,45.50.-j,43.25.Ed

*sen@nsm.buffalo.edu

I. INTRODUCTION

The problem of nonlinear energy pulse propagation in layered media is encountered in many areas of science and engineering, such as, in the use of nonlinear acoustic pulses to probe soil layers [1–14], nonlinear optical pulses in semiconductor composites [15] and in the propagation of electromagnetic pulses through the layers of the atmosphere [16]. Other applications include nonlinear acoustic pulse propagation in ocean sciences to identify different temperature zones through pulse velocity measurements [17, 18] and in areas such as non destructive evaluation of materials [19].

The existing studies typically use the wave equation where a pulse suffers significant dispersion while traveling through a medium [1, 20]. However, such an approach may not be well suited for the study of highly nonlinear and hence near ballistic propagation of short energy bursts that significantly perturb the medium and travel fast enough such that they do not rapidly disperse. Such a highly nonlinear pulse propagation regime is the focus of the mathematical analysis of the present study. Our study has been inspired by the problem of impulse propagation through shallow depths of soil beds [5–8, 12].

We start by noting recent work on nonlinear pulse propagation in granular assemblies. Granular systems are characterized by strongly nonlinear interactions between the grains [3–6, 12–14, 21–26]. Transport of a pulse can be effectively non-dispersive in problems involving soil layers, granular beds and granular alignments [7, 8, 12, 13, 21–23, 25–29]. To make our study analytically tractable, we assume that the layers are rigid. By layers we simply mean that the pulse transmission properties between any two regions may or may not be different. Thus, the case of a homogeneous bed with only one layer or of a bed with a few embedded layers is also addressed by our study. The rigidity assumption does not necessarily mean that the layers cannot move but rather that the time scale associated with movement within the layer is significantly less than the speed associated with pulse propagation. We further assume that the pulse is generated across a broad enough area such that the pulse is incident normally onto any layer. Given that we are able to vary pulse transmission properties within a layer arbitrarily, the normal incidence assumption is actually rather cosmetic and the study can be used to describe the effects of angular incidence and of lateral energy transport provided some measure of the fraction of energy transport from one layer to the next can be assessed for a given system.

Thus, here we present an exact study of pulse propagation through a rigid, layered system of infinite extent. Our model is hence effectively one dimensional. We show below that pulse propagation in our model can be related to the well known Pascal's triangle [30] and a less well known variant of the Pascal's triangle, the so-called Catalan's triangle [31–33].

We consider propagation of a single burst of energy and assume arbitrary energy transmission properties for each layer and ignore all dissipative effects. Dissipative effects can be later estimated by assuming a fixed amount of attenuation per layer and for our purposes are needed only for direct comparison with real systems (for detailed studies on this, see [34]). We present derivations of two analytic formulae to describe the backscattered energy at the surface layer as a function of time. The results agree with a numerical study of our model up to the limits of machine precision.

II. RESULTS AND DISCUSSION

The problem is set up as follows: An initial energy $E = 1$ is given to the entire first layer at time $t = 0$. We then let each rigid and infinite layer transmit a fraction of its current energy p (<1) to the next layer at time $t = 1$. By our assumption, $(1-p)$ of its current energy is retained in the first layer. The unit of time is set to be the transit time of the energy bundle from one layer to the next. We assume this transit time remains constant in our calculations. This approximation is justified in the limit of fast pulse speed compared to the time scale of the dynamics within each layer of our system [35]. At a given time step, layers can be grouped into pairs of layers coming together. In the subsequent time step these pairs reverse directions (see Fig. 1). As a result, all layers interact in each time step causing multiple incidents of energy backscattering in a given layer. In a recent study [26], when two layers came together, two energy interaction scenarios were explored (see Fig. 1). The first involved a perfect exchange of energy where two layers coming together would swap energy and then reverse direction. We call this the energy *exchange* case. The second involved an equal partitioning of the total energy in the layers coming together, where post interaction layers would leave with the average of their energies coming in. We call the second mode the *equipartition* case and this mode promotes the rapid thermalization of the energy pulses [26]. To simplify the model, we allow the depth to be infinite. This avoids the complication of having a ‘bottom wall’ where energy is lost or bounced back up in addition to whatever

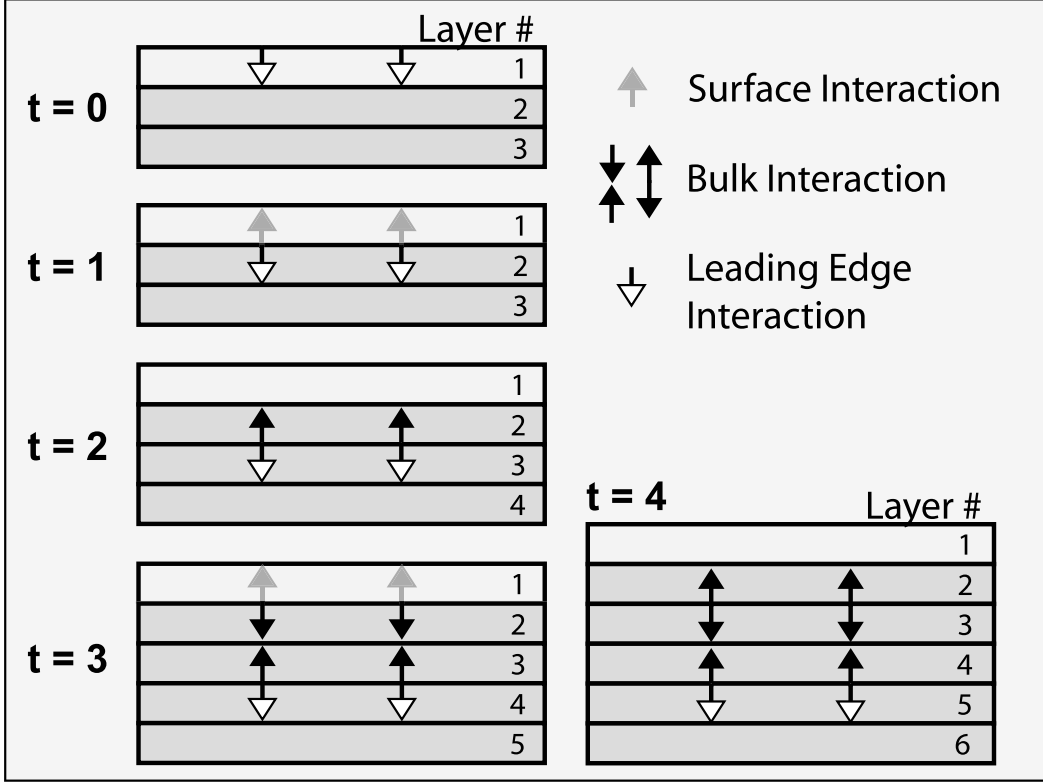


FIG. 1: Energy propagation into the layers is schematically shown.

energy is being reflected off any layer. We show the derivation of exact formulae to describe the backscattered energy at the surface layer when a pulse penetrates into a random layered system [7, 8, 12, 13, 21, 22, 28, 29]. Eq. (1) and Eq. (2), describe the backscattered energy in the exchange case. This is followed by analysis of the equipartition case, which results in Eq. (8). The formula for the equipartition case exploits the number organization of the Catalan's triangle [31–33]. We compare our results with a purely numerical study of ballistic energy propagation into a layered state with randomly varying layer transmission properties to find agreement with calculated data within the limits of machine precision.

The backscattered energy is often an experimentally measurable quantity when studying energy propagation through layered media. We hope that our exact result, in spite of being for an ideal system, becomes a helpful benchmark when interpreting backscattered quantities in layered media.

TABLE I: Propagation and backscattering in the exchange case.

t	$E_{bs}(t)$		$layer1$		$layer2$		$layer3$		$layer4$		$layer5$	\dots
0	0		1	\Rightarrow	0		0		0		0	\dots
1	0	\Leftarrow	$(1-p_1)$		p_1	\Rightarrow	0		0		0	\dots
2	$p_1(1-p_1)$		$(1-p_1)^2$	\Leftrightarrow	$p_1(1-p_2)$		p_1p_2	\Rightarrow	0		0	\dots
3	0	\Leftarrow	$p_1(1-p_2)$		$(1-p_1)^2$	\Leftrightarrow	$p_1p_2(1-p_3)$		$p_1p_2p_3$	\Rightarrow	0	\dots
4	$p_1^2(1-p_2)$		$p_1(1-p_1)(1-p_2)$	\Leftrightarrow	$p_1p_2(1-p_3)$		$(1-p_1)^2$	\Leftrightarrow	$p_1p_2p_3(1-p_4)$		$p_1p_2p_3p_4$	\dots

III. MATERIALS AND METHODS

A. Pulse Propagation in the Exchange Case

For this case, the sequence of backscattered pulses that arrive at the surface (regarded as the 0^{th} layer) defined as E_{bs} , can be tabulated as a function of t (see Table I). Recall that the exchange interaction transpires between our time steps. The “ \Leftrightarrow ” identifies the two layers that will interact in the next time step.

We ignore the terms in which $E_{bs} = 0$, and deal only with *even* t 's, i.e., by replacing t with the number N (e.g., $N = 1$ corresponds to $t = 2$). Thus, we can replace $E_{bs}(t)$ by $E_{bs}(N)$. Using Table I, $E_{bs}(N)$ can be written as

$$E_{bs}(N) = \begin{cases} p_1 f_N \Pi_1^{N-1} & N > 1 \\ p_1 f_1 & N = 1 \end{cases}, \quad (1)$$

where we use the following notation: $\Pi_1^j \equiv \prod_{i=1}^j p_i$, and $f_j \equiv (1-p_j)$. Eq. (1) implies the following recursive relation

$$E_{bs}(N+1) = \begin{cases} \frac{E_{bs}(N)f_{N+1}p_N}{f_N} & N > 2 \\ p_1^2 f_2 & N = 2 \\ p_1 f_1 & N = 1 \end{cases}. \quad (2)$$

The result in Eq. (1) generalizes the result reported in [26], where the backscattered energy sequence for constant p was shown to be $p(1-p)$, $p^2(1-p)$, $p^3(1-p)$, \dots (see terms behind the front of the energy propagation in Table I). In the absence of the bottom layer, Eq. (1) recovers the results reported in [26].

TABLE II: Description of the energy transfer process in the equipartition case. $L_i(j)$ refers to $layer_i$ at $t = j$, $E_{bs}(t)$ is the backscattered energy received back at the surface.

t	$E_{bs}(t)$		$layer1$	$layer2$	$layer3$	$layer4$	$layer5 \dots$
0	0		1	\Rightarrow 0	0	0	0 \dots
1	0	\Leftarrow	f_1	$p_1 \Rightarrow$	0	0	0 \dots
2	$p_1 f_1$		f_1^2	$\Leftrightarrow p_1 f_2$	$\Pi_1^2 \Rightarrow$	0	0 \dots
3	0	\Leftarrow	$\frac{(f_1^2 + p_1 f_2)}{2}$	$L_1(3) \Leftrightarrow$	$\Pi_1^2 f_3 \Rightarrow$	$\Pi_1^3 \Rightarrow$	0 \dots
4	$\frac{p_1}{2} (f_1^2 + p_1 f_2)$		$\frac{f_1(f_1^2 + p_1 f_2)}{2}$	$\Leftrightarrow L_3(4)$	$\frac{f_1^2 + p_1 f_2 + 2\Pi_1^2 f_3}{4} \Leftrightarrow$	$\Pi_1^3 f_4$	$\Pi_1^4 \dots$
5	0	\Leftarrow	$\frac{(f_1^2 + p_1 f_2)(2f_1 + 1) + 2\Pi_1^2 f_3}{8}$	$L_1(5) \Leftrightarrow$	$\frac{f_1^2 + p_1 f_2 + 2\Pi_1^2 f_3 + 4\Pi_1^3 f_4}{8}$	$L_3(5) \Leftrightarrow$	$\Pi_1^4 f_5 \dots$

B. Pulse Propagation in the Equipartition Case

The equipartition case exhibits a more involved pattern arising from the repeated averaging of all the middle layer energy terms, and the transfer and addition of new energy terms at the top of the chain. Table II presents the energies in the equipartition case as functions of layer number (and t).

It is difficult to succinctly record more layers in Table II without a better understanding of the patterns involved. By inspection, we can construct the expressions for E_{bs} at early times in the equipartition case. For example, we can record $E_{bs}(t = 6, N = 3)$ (equal to $p_1 \times L_1(5)$ in Table II) below,

$$E_{bs}(N = 3) = \frac{p_1}{8} \left[2f_1^3 + \Pi_1^1 f_2 + f_1^2 + 2\Pi_1^1 f_1 f_2 + 2\Pi_1^2 f_3 \right]. \quad (3)$$

However, to make further progress it is necessary to rewrite Table II with a more compact notation. We let

$$M_{\alpha, \beta} \equiv 2^{\alpha + \beta - 2} f_1^\beta \Pi_1^{\alpha - 1} f_\alpha; \quad M_{1,0} \equiv f_1, \quad \alpha \geq 1, \beta \geq 0. \quad (4)$$

The rewritten version of Table II is shown in Table III.

Let us now analyze the terms involved in Table III using three classifications of interactions: *leading edge*, *surface* and *bulk*. Leading edge interactions occur at the front of the propagating energy, and always involve a stationary layer. Surface interactions conversely occur at the zeroth layer, where we measure the backscattered energy. Finally, interactions that occur between two moving layers are considered bulk interactions.

TABLE III: Same as Table II but with improved notation

t	$E^{bs}(t)$		$layer1$	$layer2$	$layer3$	$layer4$	$layer5 \dots$
0	0		1	\Rightarrow 0	0	0	0 \dots
1	0	\Leftarrow	$M_{1,0}$	$p_1 \Rightarrow$	0	0	0 \dots
2	$p_1 M_{1,0}$		$M_{1,1}$	$\Leftrightarrow M_{2,0}$	$\Pi_1^2 \Rightarrow$	0	0 \dots
3	0	\Leftarrow	$\frac{(M_{1,1}+M_{2,0})}{2}$	$L_1(3) \Leftrightarrow$	$\frac{M_{3,0}}{2}$	$\Pi_1^3 \Rightarrow$	0 \dots
4	$\frac{p_1}{2}(M_{1,1} + M_{2,0})$		$\frac{(M_{1,2}+M_{2,1})}{4}$	$\Leftrightarrow L_3(4)$	$\frac{M_{1,1}+M_{2,0}+M_{3,0}}{4} \Leftrightarrow$	$\frac{M_{4,0}}{4}$	$\Pi_1^4 \dots$
5	0	\Leftarrow	$\frac{M_{1,2}+M_{1,1}+M_{2,1}+M_{2,0}+M_{3,0}}{8}$	$L_1(5) \Leftrightarrow$	$\frac{M_{1,1}+M_{2,0}+M_{3,0}+M_{4,0}}{8}$	$L_3(5) \Leftrightarrow$	$\frac{M_{5,0}}{8} \dots$

Since the leading edge interactions always involve a stationary layer interacting with the front of the propagating energy, they are characterized by the transmission of a Π_1^{n-1} term to a Π_1^n term, and an *opposite moving* $M_{n,0}$ term, as shown in Table III and stated in the table below.

$$\begin{array}{l}
 t_{n-1} \\
 t_n
 \end{array}
 \left\| \begin{array}{l}
 \dots \\
 \dots
 \end{array} \right.
 \left| \begin{array}{l}
 \Pi_1^{n-1} \Rightarrow 0 \quad 0 \\
 \Leftrightarrow \frac{M_{n,0}}{2^{n-2}} \quad \Pi_1^n \Rightarrow 0
 \end{array} \right.$$

The newly created, $M_{\alpha,0}$ terms at the front of the energy propagation have yet to undergo bulk interactions. The powers of two embedded in the notation therefore do not play a role at this point, and newly created leading edge terms, in the table above, have a power of two in the denominator as necessary book keeping, see Table II *layer 4* ($t = 4$), where the new $\Pi_1^3 f_4$ term of *layer 3* ($t = 4$) has a different denominator than the *layer 3* ($t = 4$) term. In Table III, the notation simplifies the expression so that *layer 4* ($t = 4$) and *layer 3* ($t = 4$) have the same denominators.

The surface interactions involve the transfer of an energy bundle through *layer 1* where it becomes measurable. A $M_{\alpha,\beta}$ term, once backscattered, becomes $p_1 M_{\alpha,\beta}$, leaving behind a $\frac{M_{\alpha,\beta+1}}{2}$ as shown in the table below. The power of two dependence is once again incorporated in the notation where once again the two in the denominator appears as book keeping.

$$\begin{array}{l}
 t \\
 t_i \\
 t_{i+1}
 \end{array}
 \left\| \begin{array}{l}
 E_{bs} \\
 0 \\
 p_1 M_{\alpha,\beta}
 \end{array} \right\|
 \left\| \begin{array}{l}
 layer1 \\
 M_{\alpha,\beta} \\
 \frac{M_{\alpha,\beta+1}}{2}
 \end{array} \right.$$

Table III reveals that the energy interactions can be expressed as linear combinations of $M_{\alpha,\beta}$ terms. Due to the nature of the bulk interactions in the equipartition case, powers of $(\frac{1}{2})$ will appear linearly with time. By factoring these out, the bulk interactions can be

TABLE IV: The Catalan structure revealed by following a $M_{2,\beta}$ term.

t	E^{bs}	$layer1$	$layer2$	$layer3$	$layer4$	$layer5$	
t_i	0	0	$p_1 \Rightarrow$	0	0	0	
t_2	0		$\Leftrightarrow M_{2,0}$	Π_1^2	\Rightarrow	0	
t_3	0	$\Leftarrow M_{2,0}$	$M_{2,0} \Leftrightarrow$		\Rightarrow	0	
t_4	$p_1 M_{2,0}$	$M_{2,1}$	$\Leftrightarrow M_{2,0}$	$M_{2,0}$	\Leftrightarrow	0	
t_5	0	$\Leftarrow M_{2,0} + M_{2,1}$	$L_1(5) \Leftrightarrow$	$M_{2,0}$	$M_{2,0}$	\Leftrightarrow	0
t_6	$p_1(M_{2,0} + M_{2,1})$	$M_{2,1} + M_{2,2}$	$\Leftrightarrow L_3(6)$	$2M_{2,0} + M_{2,1}$	\Leftrightarrow	$M_{2,0}$	$M_{2,0}$
t_7	0	$\Leftarrow 2M_{2,0} + 2M_{2,1} + M_{2,2}$	$L_1(7) \Leftrightarrow$	$3M_{2,0} + M_{2,1}$	$3M_{2,0} + M_{2,1}$	\Leftrightarrow	$M_{2,0}$
t_8	$p_1(2M_{2,0} + 2M_{2,1} + M_{2,2})$	$2M_{2,1} + 2M_{2,2} + M_{2,3}$	$\Leftrightarrow L_3(8)$	$5M_{2,0} + 3M_{2,1} + M_{2,2}$	\Leftrightarrow	$4M_{2,0} + M_{2,1}$	$4M_{2,0} + M_{2,1}$
t_9	0	$\Leftarrow 5M_{2,0} + 5M_{2,1} + 3M_{2,2} + M_{2,3}$	$L_1(9) \Leftrightarrow$	$9M_{2,0} + 4M_{2,1} + M_{2,2}$	$9M_{2,0} + 4M_{2,1} + M_{2,2}$	\Leftrightarrow	$5M_{2,0} + M_{2,1}$

reduced to simple addition of $M_{\alpha,\beta}$ terms. As we shall see, this allows for a direct view of the structure of what has been referred in the literature as Catalan's triangle [31–33].

We now choose to follow a single $M_{\alpha=a,\beta}$ term without the use of any other terms and derive a structure that will be independent of all other $M_{\alpha,\beta}$ terms. This is shown for the $M_{2,\beta}$ term in Table IV. Extracting the coefficients from a particular $M_{2,b}$ term along the diagonals in Table IV, reveals a column of the Catalan numbers in Table V.

This, however, only shows the β dependence of the Catalan numbers in the general formula. Studying Table III, one observes that to extract the time dependence, one must consider a different $M_{\alpha,0}$ term, and in doing so, begin at a different time and location in the

TABLE V: Catalan's triangle

$i \setminus j$	0	1	2	3	4	5	6
0	1						
1	1	1					
2	1	2	2				
3	1	3	5	5			
4	1	4	9	14	14		
5	1	5	14	28	42	42	
6	1	6	20	48	90	132	132

TABLE VI: The Catalan structure following a $M_{4,0}$ term, with the uncorrupted Pascal Triangle highlighted in gray. Note: All energies have been divided by $M_{4,0}$ to scale the table. X represents the locations of where terms of $\beta > 0$ have been omitted.

t	E_{bs}	<i>layer1</i>	<i>layer2</i>	<i>layer3</i>	<i>layer4</i>	<i>layer5</i>	<i>layer6</i>	<i>layer7</i>				
t_4				\Leftrightarrow	1							
t_5			\Leftrightarrow	1	1	\Leftrightarrow						
t_6		\Leftrightarrow	1	1	\Leftrightarrow	1	1	\Leftrightarrow				
t_7		\Leftarrow	1	1	\Leftrightarrow	2	2	\Leftrightarrow	1	1	\Leftrightarrow	
t_8	1	X	\Leftrightarrow	3	3	\Leftrightarrow	3	3	\Leftrightarrow	1	1	\Leftrightarrow
t_9		\Leftarrow	3	3	\Leftrightarrow	6	6	\Leftrightarrow	4	4	\Leftrightarrow	1
t_{10}	3	X	\Leftrightarrow	9	9	\Leftrightarrow	10	10	\Leftrightarrow	5	5	\Leftrightarrow
t_{11}		\Leftarrow	9	9	\Leftrightarrow	19	19	\Leftrightarrow	15	15	\Leftrightarrow	6
t_{12}	9	X	\Leftrightarrow	28	28	\Leftrightarrow	34	34	\Leftrightarrow	21	21	\Leftrightarrow

layered bed. This is done in Table VI where we follow a $M_{4,0}$, where terms involving $\beta > 0$ have been omitted.

Table VI also displays the connection between Catalan's and Pascal's triangle. Due to bulk interactions alone, the characteristic $M_{\alpha,0}$ terms propagating through time will parallel Pascal's triangle structure. In viewing a limiting case, an effectively infinitely deep layer

will undergo bulk interactions only and exactly replicate Pascal's triangle. It is when we include surface interactions, however, that we find the formation of the diagonals of Catalan's triangle as energy bundles are 'lost' from Pascal's triangle, and progressively deeper entries in Pascal's triangle become 'corrupted.' In summary, placing a wall next to Pascal's triangle will yield various diagonals of Catalan's triangle.

The above discussions show that Eq. (3), i.e., $E_{bs}(N = 3)$ can be rewritten as

$$E_{bs}(N = 3) = \frac{p_1}{2^{2(3-1)-1}} \begin{bmatrix} f_1^2 & [2^1(1)f_1 + 2^0(1)] + \\ \Pi_1^1 f_2 & [2^1(1)f_1 + 2^0(1)] + \\ \Pi_1^2 f_3 & [2^1(1)f_1^0] \end{bmatrix}. \quad (5)$$

One can write $E_{bs}(N = 4)$ as below,

$$E_{bs}(N = 4) = \frac{p_1}{2^{2(4-1)-1}} \begin{bmatrix} f_1^2 & [2^2(1)f_1^2 + 2^1(2)f_1^1 + 2^0(2)] + \\ \Pi_1^1 f_2 & [2^2(1)f_1^2 + 2^1(2)f_1^1 + 2^0(2)] + \\ \Pi_1^2 f_3 & [2^2(1)f_1^1 + 2^0(2)f_1^1 + 2^0(2)] + \\ \Pi_1^3 f_4 & [2^2(1)f_1^0] \end{bmatrix}, \quad (6)$$

and $E_{bs}(N = 5)$ as

$$E_{bs}(N = 5) = \frac{p_1}{2^{2(5-1)-1}} \begin{bmatrix} f_1^2 & [2^3(1)f_1^3 + 2^2(3)f_1^2 + 2^1(5)f_1^1 + 2^0(5)f_1^0] + \\ \Pi_1^1 f_2 & [2^3(1)f_1^3 + 2^2(3)f_1^2 + 2^1(5)f_1^1 + 2^0(5)f_1^0] + \\ \Pi_1^2 f_3 & [2^3(1)f_1^2 + 2^1(3)f_1^1 + 2^1(5)f_1^0] + \\ \Pi_1^3 f_4 & [2^3(1)f_1^1 + 2^0(3)f_1^0] + \\ \Pi_1^4 f_5 & [2^3(1)f_1^0] \end{bmatrix}. \quad (7)$$

By inspecting Eqs. (5,6,7) and the other terms, and by noting that the coefficients involved in Eqs. (5,6,7) can be captured using the number patterns in Catalan's triangle, we arrive at the following general formula, and our core result, for $E_{bs}(N)$ for $N \geq 2$, below:

$$E_{bs}(N) = \frac{p_1}{2^{2N-3}} \begin{bmatrix} f_1^2 & [2^{N-2}C_{N-2,0}f_1^{N-2} + 2^{N-3}C_{N-2,1}f_1^{N-3} + \dots + 2^1C_{N-2,N-3}f_1^1 + 2^0C_{N-2,N-2}f_1^0] + \\ \Pi_1^1 f_2 & [2^{N-2}C_{N-2,0}f_1^{N-2} + 2^{N-3}C_{N-2,1}f_1^{N-3} + \dots + 2^1C_{N-2,N-3}f_1^1 + 2^0C_{N-2,N-2}f_1^0] + \\ \Pi_1^2 f_3 & [2^{N-2}C_{N-2,0}f_1^{N-3} + 2^{N-3}C_{N-2,1}f_1^{N-4} + \dots + 2^1C_{N-2,N-3}f_1^0] + \\ \vdots & \vdots \\ \Pi_1^{N-2} f_{N-1} & [2^{N-2}C_{N-2,0}f_1^1 + 2^{N-3}C_{N-2,1}] + \\ \Pi_1^{N-1} f_N & [2^{N-2}C_{N-2,0}] \end{bmatrix}. \quad (8)$$

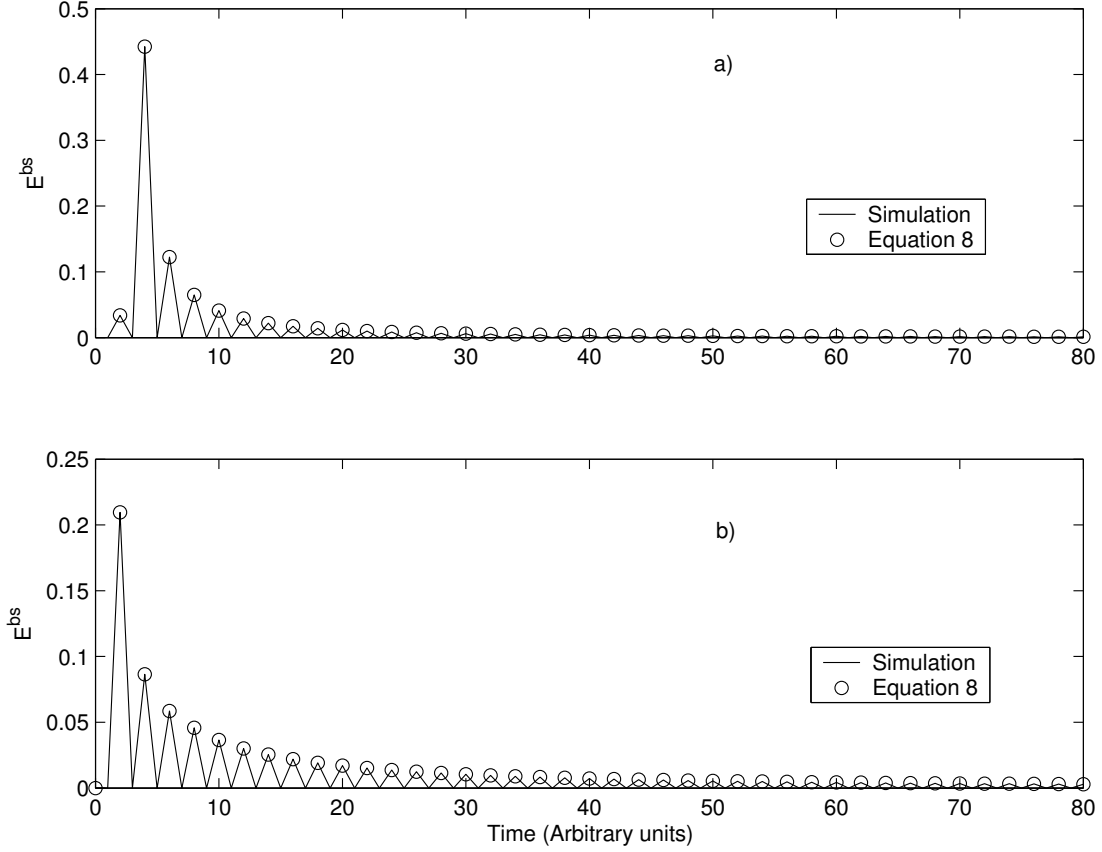


FIG. 2: Comparison between the numerical result and the analytically obtained result reveals perfect agreement for two distinct realizations of $\{p_j\}$ s for the equipartition case.

where the values $C_{i,j} = \frac{(i+j)!(i-j+1)}{j!(i+1)!}$, are from Catalan's triangle [31–33], and $E_{bs}(1) = p_1 f_1$. From Equation (8) and the Catalan numbers we see that *contributions of backscattered energy do not necessarily taper off with depth. All levels previously reached by the propagating energy as well as those at the front are equally important.*

To establish that Eq.(8) correctly describes the backscattered energy in our problem, we compare data on $E_{bs}(N)$ generated via analytic formula and numerical calculations of the model for the same randomly generated sequence p_i where i varies from 1 to N for two specific sets of $\{p_i\}$. This is shown in Figs. 2 (a) and (b). Our data reveals agreement between the numerical and analytical data within the limits of computational error and hence confirms the correctness of Eq. (8).

C. Connection with Anderson Localization

Anderson localization describes the exponential localization of eigenstates for a wave equation with a disordered potential field [36–38]. Studies by McKenna *et al.*, Hopkins *et al.* and others [39–41] experimentally validate that in wave propagation problems where the propagation of a perturbation is governed by the wave equation, Anderson localization survives the presence of “weak” nonlinearity and disorder. By “weak” nonlinearity it is assumed that the length scale across which nonlinear effects are dominant must be greater than the length scale associated with Anderson localization. In the present study, while there is disorder, there is no natural localization of the propagating pulse due to that disorder. This is because the highly nonlinear ballistic pulse propagation in the present model is such that energy cannot get trapped between the layers and hence, in effect, the length scale associated with nonlinearity acts across a length scale of one layer, which is the minimum meaningful distance in the study. The random variation in transmission of energy on the other hand is not designed to localize the incoming pulse but rather allows slowing down or enables easier passage of the pulse as it propagates through one or more layers. Regardless of whether exchange or equipartition cases are considered, the role of nonlinearity in the present analysis is strong compared to effects of disorder.

Acknowledgments: This research has been partially supported by the Army Research Office.

-
- [1] L.H.T. Le, R. Burridge, CREWES Research Rept. 4 (1992)16-1.
 - [2] J.-F. Clouet, J.-P. Fouque, *Wave Motion* 25 (1997)361.
 - [3] S. R. Hostler, C.E. Brennen, *Phys. Rev. E* 72 (2005) 031303.
 - [4] S. R. Hostler, C.E. Brennen, *Phys. Rev. E* 72 (2005) 031304.
 - [5] G.S. Baker, C. Schmeissner, D.W. Steeples, R.G. Plumb, *Geophys. Res. Lett.* 26 (1999) 279.
 - [6] G.S. Baker, D.W. Steeples, C. Schmeissner, M. Pavlovic, R.G. Plumb, *Geophys. Res. Lett.* 28 (2001) 627.
 - [7] A.J. Rogers, C.G. Don, *Acoustics Australia* 22 (1994) 5.
 - [8] S. Swaminathan, D.P. Visco, Jr. and S. Sen, *Appl. Phys. Lett.* 90 (2007) 154107.
 - [9] S.A. Solin, H. Zabel, *Adv. Phys.* 37 (1988) 87.

- [10] S. Auerbach, K.A. Carrado, P.K. Dutta (Eds.) Handbook of Layered Materials, Marcel Dekker, New York, 2004.
- [11] J.R. Dutcher, A.G. Marangoni (Eds.) Soft Materials: Structure and Dynamics, CRC Press, Boca Raton, 2004.
- [12] A. Shukla, C. Damania, *Exper. Mech.* 27 (1987) 268.
- [13] C.Y. Zhu, A. Shukla, M.H. Sadd, *J. Appl. Mech.* 58 (1991) 341.
- [14] N. Rawlinson, M. Stambridge, *Geophys.* 69 (2004) 1338.
- [15] N. Finlayson, E.M. Wright, G.I. Stegeman, *IEEE J. Quant. Electr.* 26 (1990) 770.
- [16] J.H. Yee, R.A. Alvarez, D.J. Mayhall, D.P. Byrne, J. DeGroot, *Phys. Fluids.* 29 (1986) 1238.
- [17] P.J. Sutton, P.F. Worcester, G. Masters, B.D. Cornuelle, J.F. Lynch, *J. Acoust. Soc. Amer.* 94 (1993) 1517.
- [18] A.B. Baggeroer, T.G. Birdsall, C. Clark, J.A. Colosi, B.D. Cornuelle, D. Costa, B.D. Dushaw, M. Dzieciuch, A.M.G. Forbes, C. Hill, B.M. Howe, J. Marshall, D. Menemenlis, J.A. Mercer, K. Metzger, W. Munk, R.C. Spindel, D. Stammer, P.F. Worcester, C. Wunsch, (ATOC Consortium), *Science* 281 (1998) 1327.
- [19] J. Vollmann, D.M. Profunser, A.H. Meier, M. Döbeli, J. Dual, *Ultrasonics* 42 (2004) 657.
- [20] S.I. Rokhlin, L. Wang, *J. Acoust. Soc. Amer.* 112 (2002) 822.
- [21] R.S. Sinkovits, S. Sen, *Phys. Rev. Lett.* 74 (1995) 2686.
- [22] S. Sen, R.S. Sinkovits, *Phys. Rev. E* 54 (1996) 6857.
- [23] G. Ben Dor, A. Britan, T. Elperin, O. Igra, J. Jiang, *Exper. Fluids* 22 (1997) 432.
- [24] M.F. Hamilton, D.T. Blackstock (Eds.) *Nonlinear Acoustics*, Academic, San Diego, 1998.
- [25] K. van Wijk, M. Haney, J.A. Scales, *Phys. Rev. E* 69 (2004) 036611.
- [26] T.R. Krishna Mohan, S. Sen, *Phys. Rev. E* 67 (2003) 060301(R).
- [27] V.F. Nesterenko, *Dynamics of Heterogeneous Materials*, Springer, New York, 2001.
- [28] M.J. Naughton, R.S. Shelton, S. Sen, M. Manciu, *IEE Conf. Publ.* 458 (1998) 249.
- [29] S. Sen, T.R. Krishna Mohan, D.P. Visco, S. Swaminathan, A. Sokolow, M. Nakagawa, *Int. J. Mod. Phys. B* 19 (2005) 2951.
- [30] B. Pascal, *Oeuvres complètes*, Seuil, Paris, 1960.
- [31] L.W. Shapiro, *Discrete Math.* 14 (1976) 83.
- [32] D.G. Rogers, *Discrete Math.* 22 (1978) 301.
- [33] D.N. Kreher, S.R. Stinson, *Combinatorial algorithms, generation, enumeration and search*

- (CAGES), CRC, Boca Raton, 1998, p. 95.
- [34] M. Manciu, S. Sen, A.J. Hurd, *Physica D* 157 (2001) 226.
- [35] D.P. Visco, S. Swaminathan, T.R. Krishna Mohan, A. Sokolow, S. Sen, *Phys. Rev. E* 70 (2004) 051306.
- [36] P.W. Anderson, *Phys. Rev.* 109 (1958) 1492.
- [37] A. Ishimaru, *Wave Propagation and Scattering in Random Media* (Academic, New York, 1978).
- [38] V.K. Varadan, T. Ma and V.V. Varadan, *J. Acoust. Soc. Am.* 77 (1985) 375.
- [39] M.J. McKenna, R.L. Stanley and J.D. Maynard, *Phys. Rev. Lett.* 69 (1992) 1807.
- [40] V.A. Hopkins, J. Keat, G.D. Meegan, T. Zhang and J.D. Maynard, *Phys. Rev. Lett.* 76 (1996) 1102.
- [41] A. Tourin, A. Derode, A. Peyre and M. Fink, *J. Acoust. Soc. Am.* 108 (2000) 503.